



## Hydraulic resistance of submerged rigid vegetation derived from first-order closure models

Davide Poggi,<sup>1</sup> Claudia Krug,<sup>2</sup> and Gabriel G. Katul<sup>2,3</sup>

Received 19 August 2008; revised 5 June 2009; accepted 23 June 2009; published 30 October 2009.

[1] The past decade witnessed rapid developments in remote sensing methods that now permit an unprecedented description of the spatial variations in water levels ( $H_w$ ), canopy height ( $h_c$ ), and leaf area density distribution ( $a$ ) at large spatial scales. These developments are now renewing interest in effective resistance formulations for water flow within and above vegetated surfaces so that they can be incorporated into simplified water routing models driven by such remote sensing products. The first generation of such water routing models linked the bulk velocity to gradients in  $H_w$  via a constant diffusion velocity that cannot be inferred from canopy properties ( $a$  and  $h_c$ ). The next generation of such hydrologic models must preserve the nonlinear relationship between the resistance value, canopy attributes (e.g.,  $a$  and  $h_c$ ), and  $H_w$  without compromising model simplicity. Using a simplified scaling analysis on the depth-integrated mean momentum balance and a two-layer model for the bulk velocity, the Darcy-Weisbach friction factor ( $f$ ) was shown to vary with three canonical length scales that can be either measured or possibly inferred from remote sensing products  $H_w$ ,  $h_c$ , and the adjustment length scale  $L_c = (C_d a)^{-1}$ , where  $C_d$  is the drag coefficient (of order unity). The scaling analysis proposed here reveals that these length scales can be combined in two dimensionless groups,  $H_w/h_c$  and  $L_c/h_c$ . The dependence of  $f$  on these two functional groups was then explored using a combination of first-order closure modeling and 130 experimental runs derived from a large number of flume experiments carried out for rigid and flexible vegetation. The results from the data and the model show a nonlinear decrease in  $f$  with increasing  $H_w/h_c$  at a given  $L_c/h_c$  and the nonlinear increase in  $f$  with decreasing  $L_c/h_c$ . Furthermore, both model and data results did not exhibit any dependence on the bulk Reynolds number.

**Citation:** Poggi, D., C. Krug, and G. G. Katul (2009), Hydraulic resistance of submerged rigid vegetation derived from first-order closure models, *Water Resour. Res.*, 45, W10442, doi:10.1029/2008WR007373.

### 1. Introduction

[2] Continental-scale water cycle models that rely on water level changes in the main channel or floodplain are now receiving significant attention given the societal need to quantify the sustainability of existing fresh water resources. This renewed interest is also due to the recent developments in satellite radars that allow an accurate measure of the surface water levels of large basins [Alsordf *et al.*, 2000, 2003, 2007a, 2007b; Alsordf and Lettenmaier, 2003]. For example, satellite interferometric synthetic aperture radars (SAR) were reportedly able to sample stage elevations to within a centimeter at roughly a 100 m planar resolution in large ( $\sim 10,000$  km<sup>2</sup>) floodplains thereby motivating the development of refined large-scale hydrodynamic models that describe changes in water storage ( $S_w$ ). These models

must be limited in parameterization yet must adequately describe broad features of the floodplain drainage over large spatial domains. Given such scale constraints, the use of computationally demanding three-dimensional hydrodynamic flow models for predicting water level and discharge becomes prohibitive.

[3] Recent modeling efforts at such large scales (i.e., scales comparable to the SAR planar sampling resolution) focused on using the mean continuity equation [Alsordf *et al.*, 2005, 2007a], given by

$$\frac{\partial S_w}{\partial t} = \frac{\partial Q_i}{\partial x_i} + A(P - E - I), \quad (1)$$

where  $S_w$  can be determined from SAR via temporal sampling,  $t$  is time,  $Q_i$  is the flow rate along directions  $x_i$  (i.e.,  $x_1 = x$  and  $x_2 = y$  are the planar coordinates),  $A$  is the planar area,  $P$  is the precipitation,  $E$  is evapotranspiration, and  $I$  is infiltration. Since  $Q_i$  cannot be directly measured, a model relating  $Q_i$  to the water depth ( $H_w$ ), must be employed in such a framework. The formulations currently used at such large scales are based on a linear diffusive representation of  $Q_i$ , given as

$$Q_i = -DH_w \frac{\partial H_w}{\partial x_i}, \quad (2)$$

<sup>1</sup>Dipartimento di Idraulica, Trasporti ed Infrastrutture Civili, Politecnico di Torino, Turin, Italy.

<sup>2</sup>Department of Civil and Environmental Engineering, Duke University, Durham, North Carolina, USA.

<sup>3</sup>Nicholas School of the Environment and Earth Sciences, Duke University, Durham, North Carolina, USA.

where  $D$  is treated as an empirical diffusion velocity coefficient. This approach revises existing continental-scale water cycle models that instantly propagate water level changes across the floodplain to one where this change propagates as a diffusive process. This diffusive representation captured the fundamental behavior of recessional flow as measured by satellite interferometric SAR, and has provided first-order estimates of  $D$  for two large Amazonian floodplains that ranged from 6,000 to 13,000 km d<sup>-1</sup> (70 m s<sup>-1</sup> – 150 m s<sup>-1</sup>), impressively high conductivities.

[4] An alternative approach to modeling  $Q_i$ , without loss in simplicity or added parameters, is to use the classical open channel flow equations. In fact, upon representing the cross-sectional averaged velocity ( $U_b$ ) by a standard formulation such as Darcy-Weisbach equation (or variants on it), given as

$$U_{b,i} = \sqrt{\frac{8}{f}} \cdot (g H_w S_i)^{1/2}, \quad (3)$$

then

$$Q_i \cong \sqrt{\frac{8}{f}} \cdot L H_w^{3/2} \left( \frac{\partial H_w}{\partial x_i} \right)^{1/2}, \quad (4)$$

where  $f$  is Darcy-Weisbach's roughness coefficient,  $L$  is a characteristic width, and  $S_i$  is the energy grade line slope estimated here as  $\partial H_w / \partial x_i$  for locally uniform flow. When equation (2) is combined with equation (4), it is clear that  $D$  must be given by  $D = (8H_w/f)^{1/2} L (\partial H_w / \partial x_i)^{-1/2}$ . SAR data can still be used to estimate  $D$  provided  $f$  is known. Hence, the main challenge to the next generation of such hydrologic models is whether  $f$  can be linked to “measurable” canopy and flow attributes via remote sensing approaches, the subject of this work. Other steady uniform flow formulations, such as the Manning's friction factor ( $n$ ) can also be used to replace  $D$ . A practical advantage to formulating water flow rates using a standard open channel equation are twofold: (1) such resistance equations have a long history of describing bulk velocities reasonably well in surface flows and ensure that the intrinsic nonlinearities in the  $Q_i$  versus  $H_w$  are preserved, and (2) on the monitoring side, they hold promise for the possibility of combining SAR data with canopy light detection and ranging (lidar) data, now capable of measuring canopy height ( $h_c$ ), and leaf area density ( $a$ ), both variables known to impact the friction factor  $f$  in addition to  $H_w$ . Various flume and field studies have already shown that  $n$  and  $f$  depend on the drag coefficient ( $C_d$ ) imposed by the vegetation,  $a$ ,  $H_w$ , and  $h_c$  as well as the bulk Reynolds number [Baptist, 2003; Carollo et al., 2002; Helmers and Eisenhauer, 2006; Helmio, 2002; Jarvela, 2002; Musleh and Cruise, 2006; Shi et al., 1995; Stone and Shen, 2002; Tsihrintzis and Madiedo, 2000; Wilson et al., 2003]. General formulations linking all these variables to resistance factors remain the subject of active research, especially in submerged canopies, and their potential use in continental-scale hydrologic models (e.g., an estimate of  $D$ ) provides additional motivation for progress. Historically, these formulations have been partially “encoded” in the so-called “retardance curves” that show how  $n$  (or  $f$ ) varies

with bulk Reynolds number (or  $U_b H_w$ ) for a number of vegetation flexibility indices [Chow, 1959].

[5] Using basic canopy turbulence theories and the wealth of flume experiments acquired over the past three decades, it is demonstrated here that  $f$  (or  $n$ ) can be related to dimensionless functions represented by  $C_d$ ,  $a$ ,  $h_c$ , and  $H_w$  using a simplified scaling analysis. Models that employ first-order closure principles for rigid and submerged canopies are then used to functionally link these dimensionless groups to  $f$  (or  $n$ ). Exploring rigid canopies is a logical starting point for any extension to the more complex case of flexible canopies or to situations where topographic variations can dramatically alter the mean flow dynamics [Poggi and Katul, 2007a, 2007c; Poggi et al., 2007]. Even within this restrictive scope, numerous simplifying assumptions about the momentum transfer within the canopy are needed. With these assumptions, bulk flow calculations are evaluated using first-order closure formulations and a wide range of data sets already published.

## 2. Theory

[6] For a stationary and planar homogeneous flow, the time and planar-averaged mean momentum equation along the longitudinal direction is given by

$$0 = g S + \frac{\partial \tau}{\partial z} - \frac{1}{2} \delta_{sf} C_d a \bar{U}^2, \quad (5)$$

where  $\tau$  is the total stress per unit density and combines the molecular ( $\tau_m$ ) and turbulent ( $\tau_t = \overline{u'w'}$ ) shear stresses,  $\overline{u'w'}$  is the momentum turbulent flux (m<sup>2</sup> s<sup>-2</sup>),  $z$  is the vertical direction, and  $\delta_{sf}$  is the Heaviside step function given by

$$\delta_{sf} = \begin{cases} 1 & z/h \leq 1 \\ 0 & z/h > 1. \end{cases}$$

While it is not the intend here to show how this equation was formally derived from time and volume averaging the longitudinal momentum balance [Finnigan, 2000; Lopez and Garcia, 2001; Nikora et al., 2001; Raupach and Shaw, 1982; Shimizu and Tsunimoto, 1994], it is important to point out a few key approximations invoked. In particular, equation (5) neglects dispersive fluxes and finite porosity effects. Dispersive fluxes appear to be small in dense canopies, at least in relation to  $\overline{u'w'}$ , but not in sparse canopies [Cheng and Castro, 2002; Poggi et al., 2004a; Poggi and Katul, 2008a, 2008b; Pokrajac et al., 2007]. Notwithstanding all these limitations, this simplified budget remains a reference starting point for exploring the main objective here.

### 2.1. Basic Scaling Analysis

[7] An effective resistance formulation can be derived by considering the depth-averaged mean momentum balance after neglecting the molecular stresses (relative to turbulent stresses), resulting in

$$0 = \int_0^{H_w} g S dz + \overline{u'w'}(H_w) - \overline{u'w'}(0) - \frac{1}{2} \int_0^{h_c} C_d a [\bar{U}(z)]^2 dz. \quad (6)$$

The stress  $\overline{w'u'}$  ( $H_w$ )  $\approx 0$  in the absence of any surface wind effects. Furthermore,  $\overline{w'u'}$  (0)  $\approx 0$  within dense canopies

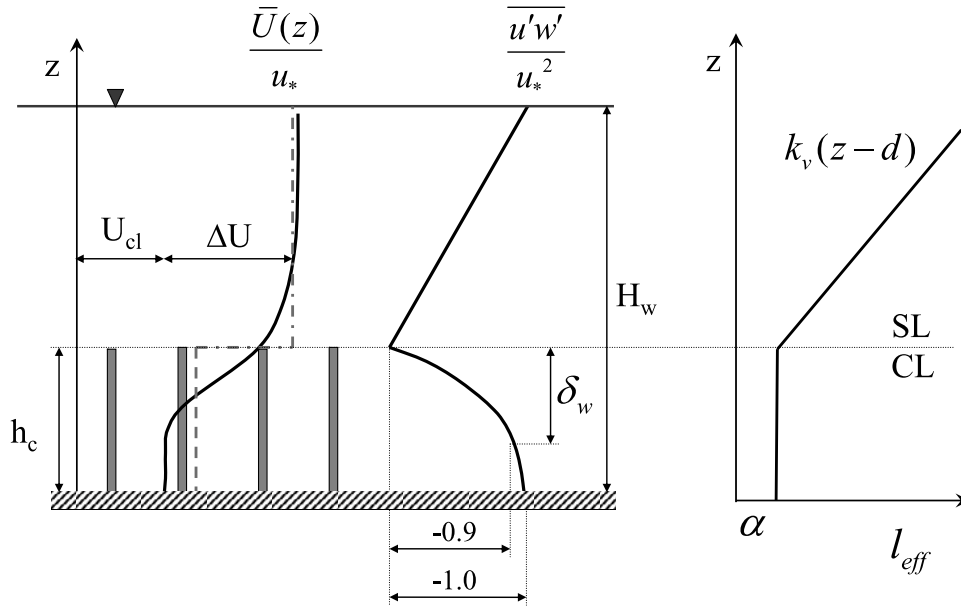


**Figure 1.** Schematic representation of the two-layer mixing length model ( $l_{eff}$ ) inside the canopy layer and in the surface layer, canonical profiles of the mean velocity  $\bar{U}/u_*$  and turbulent stresses  $(\overline{u'w'}/u_*^2)$ , and the definition of the penetration depth  $\delta_w$ . The two-layer bulk velocity approximation to the  $\bar{U}/u_*$  profile, with  $U_{cl}$  being the bulk velocity in the CL and  $U_{cl} + \Delta U$  being the bulk velocity in the SL, is also shown as dashed lines. Note the continuity in the mixing length at the canopy top, the basis for defining  $\alpha$ .

given that much of the momentum absorption occurs within the canopy volume. Hence, when  $C_d a$  does not appreciably vary with  $z$  (at least relative to  $\bar{U}$ ), the integrated mean momentum balance can be approximated as

$$g S H_w = \frac{1}{2} C_d a \int_0^{h_c} [\bar{U}(z)]^2 dz. \quad (7)$$

Hypothetically, if  $\bar{U}(z) = U_b$  and is invariant with variations in  $z$ , the above equation reduces to

$$g S H_w = \frac{1}{2} C_d a h_c U_b^2. \quad (8)$$

For these idealized conditions, the Darcy-Weisbach friction factor  $f$  (or  $n$ ) can be related to the canopy attributes via

$$\frac{8}{f} = \frac{U_b^2}{u_*^2} = \frac{2}{C_d a h_c} = 2 \frac{L_c}{h_c}. \quad (9)$$

Here,  $u_* \approx \sqrt{g S H_w}$  is the friction velocity (at the canopy top). Hence, when the velocity is uniform with depth,  $f$  is independent of  $H_w$  and only varies with the adjustment length  $L_c = (C_d a)^{-1}$  and the canopy height, which can be combined into a dimensionless group ( $L_c/h_c$ ) [Baptist et al., 2007; Huthoff et al., 2007]. Because  $f$  is independent of  $H_w$  and only depends on canopy attributes (vis à vis  $n$  that varies with  $H_w$ ), it is a convenient starting point for any scaling analysis that must account for the effects of depth-variable mean velocity. Note also that for a constant  $C_d a$  (assumed to be independent of  $U_b$ ) and  $h_c$ ,  $f$  is also a constant independent of

the bulk Reynolds number. However, a large number of experiments have already shown that  $f$  is strongly dependent on the submergence depth ( $H_w/h_c$ ) and can vary with the bulk Reynolds number ( $\sim U_b H_w$ ) [Green, 2005; Jarvela, 2002; Kirby et al., 2005; Tsihrintzis and Madiedo, 2000; Wilson and Horritt, 2002; Wu et al., 1999]. This Reynolds number dependence is expected when the viscous drag is not negligible, or when the canopy is flexible so that its effective height and leaf area become dependent on the flow velocity.

[8] Contrary to the assumption that  $\bar{U}(z) = U_b$ ,  $\bar{U}(z)$  is known to strongly vary with  $z$ , especially within the canopy (see Figure 1). A first-order correction to the constant  $U_b$  assumption across the entire domain is to decompose the mean velocity profile into two regions: a canopy layer [Nikora et al., 2004] and a surface layer, each having their own characteristic bulk velocity. Hence, the bulk velocity can be decomposed into a linear superposition of two constant velocities within each of these regions, given by

$$U_b = U_{cl} + (1 - \lambda)\Delta U; \quad \text{where } \lambda = \frac{h_c}{H_w}, \quad U_{sl} = \Delta U + U_{cl}, \quad (10)$$

where  $U_{cl}$  is the bulk velocity in the canopy layer,  $U_{sl}$  is the bulk velocity in the surface layer, and  $\lambda$  is the reciprocal of the submergence depth. For this two-layer velocity decomposition, the integrated mean momentum balance becomes

$$U_{cl}^2 = \frac{u_*^2}{\frac{1}{2} C_d a h_c},$$

and  $f$  is now given by

$$\frac{8}{f} = \frac{(U_{cl} + (1 - \lambda)\Delta U)^2}{u_*^2} = \frac{U_{cl}^2(1 + (1 - \lambda)\Delta U/U_{cl})^2}{u_*^2} \\ = 2 \frac{L_c}{h_c} \left( 1 + \left( 1 - \frac{H_w}{h_c} \right) \frac{\Delta U}{U_{cl}} \right)^2. \quad (11)$$

Note that when  $\Delta U = 0$  (i.e., constant mean velocity profile),  $f = 2L_c/h_c$  is recovered.

[9] It is clear that even for such a two-layer model comprising only two bulk velocities, the coupling between  $U_{cl}$  and  $\Delta U$  as well as the submergence depth become important. Some experiments for vegetation comprising cylinders suggested that  $\Delta U/U_{cl}$  may be linearly correlated with the product of  $a$  and the cylinder diameter ( $d$ ) [Ghisalberti and Nepf, 2004; Nepf et al., 2007]. When such a correlation is assumed in the above expression for  $f$ , it follows that  $f$  must only vary with submergence depth and canopy features (e.g.,  $C_d$ ,  $a$ ,  $d$ , and  $h_c$ ) and does not vary with variations in local velocity except in the case when  $C_d$  varies with  $U_{cl}$  or in the case of flexible vegetation. Hence, the above scaling analysis is suggestive that any exploration of  $f$ , even for a rigid canopy at high Reynolds number, must account for at least two dimensionless groups:  $L_c/h_c$  and  $H_w/h_c$ .

[10] Experimentally, it is necessary to conduct detailed measurements across a prohibitively large set of conditions to arrive at the precise functional form between  $f$  and these two dimensionless groups. One approach is to attempt to synthesize the data from most of the experiments carried out on rigid and flexible vegetation. Such a data set is very large but still not large enough to cover all the possible combinations of  $L_c/h_c$  and  $H_w/h_c$ . Moreover the data set suffers from intrinsic variability in data collection modality, canopy type, and experimental facilities. Hence, to overcome this deficiency, it may be possible to extend the range of  $L_c/h_c$  and  $H_w/h_c$  via model calculations. Closure models, when appropriately parameterized (say by the limited data sets), may suffice to infer the behavior of  $f$  across a wide range of  $L_c/h_c$  and  $H_w/h_c$  starting from the basic momentum balance. In section 2.2, the basic principles of such a simple yet robust first-order closure model is briefly reviewed. To be clear, by simple we mean that the approach here does not require “extra” closure constants beyond what was needed in the scaling analysis (when compared to higher-order closure modeling). By robust, we mean that the closure assumption is not sensitive to the precise configuration of the canopy elements.

## 2.2. Closure Model

[11] The first-order closure approach models the turbulent stress via an eddy viscosity using

$$\tau = -(v_t + v_m) \frac{\partial \bar{U}}{\partial z} \\ v_t = l_{eff} U_{eff}, \quad (12)$$

where  $v_t$  and  $v_m$  are the turbulent and molecular viscosities ( $\text{m}^2 \text{s}^{-1}$ ), and  $l_{eff}$  (m) and  $U_{eff}$  ( $\text{m s}^{-1}$ ) are the effective mixing length and velocity scale, respectively. Estimates or phenomenological models of these two variables, especially inside the canopy layer, are required. Other models such as

the  $k - \omega$  [Lopez and Garcia, 2001; Neary, 2003], or  $k - \varepsilon$  [Baptist et al., 2007; Defina and Bixio, 2005] can also be used in lieu of the first-order closure approach above, where  $k$  is the turbulent kinetic energy (TKE),  $\varepsilon$  is the TKE dissipation rate, and  $\omega$  is the specific dissipation rate. The  $k - \omega$  and  $k - \varepsilon$  models include, in addition to the mean momentum budget, budget equations for  $k$  and  $\varepsilon$ . Modeling the effect of vegetation on the production and destruction terms of  $k$  and  $\omega$  (or  $\varepsilon$ ) require additional phenomenological models for these source-sink terms, often at the same level of heuristic assumptions as the closure model for  $\tau$ . Furthermore, the number of closure constants needed in  $k - \omega$  and  $k - \varepsilon$  models is greater than four. Thus, it is likely that the added complexity in these models does not justify the improved predictive skill, at least if the model is intended to reproduce  $U_b$  (the objective here). This has been demonstrated for a wide range of terrestrial vegetation with complex canopy morphology [Katul et al., 2004]. Defina and Bixio [2005] also compared first-order closure model calculations with  $k - \varepsilon$  calculations and found good agreement between the two calculations for  $\bar{U}$ . For these reasons, it suffices to use first-order closure modeling for deriving effective resistance parameterization that requires  $U_b$ .

[12] The simplest approach to specifying an effective length and velocity scale in first-order closure modeling is to retain the decomposition of the flow domain into a surface layer (SL) and a canopy layer (CL). In the SL, it is common to assume a logarithmic mean velocity profile with a virtual zero point situated inside the canopy at  $z = d_o$  (hereafter referred to as the zero-plane displacement height). Hence, for the SL,

$$l_{eff}^{sl} = k_v(z - d_o) \text{ and } U_{eff}^{sl} = l_{eff}^{sl} \left| \frac{\partial \bar{U}}{\partial z} \right|, \quad (13)$$

where  $k_v = 0.4$  is the Von Karman constant.

[13] For the CL, a number of models have been proposed for  $l_{eff}$  but we focus on two of them. One of these models considers explicitly the effect of  $H_w$  on  $l_{eff}$ , while the other only considers this effect implicitly. When  $H_w/h_c$  is of order unity, boundary layer vortices forming above the canopy may be constrained by the water surface [e.g., Nepf et al., 2007] and this constraint may impact their momentum transport efficiency. It is for this reason that some mixing length models inside the canopy consider  $H_w$ . One such model proposes that  $U_{eff}^{cl} = \bar{U}$  and

$$\frac{l_{eff}^{cl}}{h_c} = 0.0144 \sqrt{\frac{H_w}{h_c}}. \quad (14)$$

The above effective mixing length is entirely empirical and was derived by Meijer and Van Velzen [1999] (hereinafter referred to as MV99) by comparing measured and computed mean velocity profiles in a large flume facility and across many experimental runs [Meijer and Van Velzen, 1999]. MV99 carried out more than 50 tests by varying  $h_c$  (steel bars),  $a$ , and the energy gradients (i.e.,  $S$ ) systematically to arrive at this expression. Because of differences in eddy viscosity formulations in the SL and CL here, the transition zone between SL and CL for the MV99 model is not based on  $h_c$  but is based on enforcing continuity in  $v_t$ . This continuity in  $v_t$  may lead to a switch between CL and SL that is not at  $z/h_c = 1$ .

[14] The second approach to formulating  $l_{eff}^v$  is to retain the same effective velocity as in the SL, (i.e.,  $U_{eff} = l_{eff} \left| \frac{\partial \bar{U}}{\partial z} \right|$ ), but define  $l_{eff} = \alpha h_c$ , where  $\alpha$  needs to be determined. Some studies suggested that the continuity in the mixing length at the transition zone between the CL and SL be used to estimate  $\alpha$  [Katul *et al.*, 2004]. Katul *et al.* [2004] argued that in a deep boundary layer above terrestrial vegetation, matching the two mixing lengths at  $z/h_c = 1$  results in  $\alpha = k_v (1 - d_o/h_c)$ .

[15] This formulation remains incomplete because  $d_o/h_c$  is not a priori known. However,  $d_o/h_c$  can be implicitly related to  $\bar{U}$  by assuming that  $d_o$  is collocated with the centroid of the drag force imposed by the vegetation on the fluid [Jackson, 1981; Thom, 1971]. This assumption yields an estimate of  $d_o$  and  $\alpha$  given by

$$d_o = \frac{\int_0^{h_c} z \left( \frac{1}{2} C_d a \bar{U}^2 \right) dz}{\int_0^h \left( \frac{1}{2} C_d a \bar{U}^2 \right) dz}; \quad \alpha = k_v \left[ 1 - \frac{1}{h_c} \frac{\int_0^{h_c} z \left( \frac{1}{2} C_d a \bar{U}^2 \right) dz}{\int_0^h \left( \frac{1}{2} C_d a \bar{U}^2 \right) dz} \right]. \quad (15)$$

Note that this definition of  $\alpha$  becomes independent of  $C_d a$  when  $C_d a$  does not vary with  $z$ . If much of the momentum flux is extracted near the top of the canopy, then  $\alpha$  will be small. Typical values of  $\alpha$  for dense vegetation are around 0.08 assuming a  $d/h_c \approx 0.8$  [Nepf *et al.*, 2007]. In terrestrial ecosystems, however,  $d/h_c = 0.65-0.70$  resulting in  $\alpha \approx 0.15$ , almost double its aquatic counterpart. Because  $l_{eff}$  depends in a nonlocal manner on the  $\bar{U}(z)$  profile, this approach requires an iterative solution to the mean momentum balance to arrive at  $\bar{U}(z)$ . If the variations in  $C_d$  with  $\bar{U}$  are known (or can be modeled), and if the vertical distribution of  $a(z)$  is measured, then the proposed  $\alpha$  formulation can still be used without modifications. The  $\alpha$  is also related (but not identical) to the so-called penetration depth ( $\delta_w$ ), defined as the distance between the top of the canopy and the point within the canopy at which  $|u'w'|$  decays to 10% of its maximum value [Nepf and Vivoni, 2000].

[16] Finally, the choice of specifying a two-layer mixing length rather than a two-layer eddy viscosity as done in recent studies [White and Nepf, 2008] can be justified on less objectionable theoretical grounds. A continuous but non-differentiable mixing length at the canopy top guarantees that the nonsmoothness is entirely due to a discontinuity imposed by a canopy/no-canopy transition on eddy sizes. Moreover, Finnigan and Belcher [2004] showed that a variant of this first-order closure used here can be viewed as the proper theoretical limit of a second-order turbulence closure scheme when the turbulent transport terms are progressively neglected and can be justified as a reasonable approximation provided the canopy density does not change rapidly with height (as is assumed here).

[17] Two boundary conditions are necessary to solve the mean momentum balance for  $\bar{U}(z)$  [Defina and Bixio, 2005; Lopez and Garcia, 2001; Poggi *et al.*, 2004c]:

$$d\bar{U}/dz = 0 \text{ at } z = H_w$$

(i.e., no momentum flux crossing the free surface) and

$$\bar{U} = \sqrt{\frac{2gS}{C_d a}} \text{ at } z = 0$$

(i.e.,  $d\bar{u}'w'/dz = 0$  or a free slip condition).

[18] The upper boundary condition can be revised to permit wind effects to be incorporated if they are known. The lower-boundary condition assumes that in dense canopies, much of the momentum has already been extracted near the ground (as is expected when  $\delta_w < h_c$ ) so that the mean momentum balance is primarily between the drag force and the component weight of the fluid. This region, not surprisingly, is often labeled as the pressure-driven region. For sparse canopies, this approximation is more questionable on theoretical grounds, though experiments and model results of Poggi *et al.* [2004c] suggest reasonably good agreement between data and model calculations using this free slip condition once a small distance ( $\sim 10\%$ ) away from the  $z = 0$  boundary is exceeded.

### 3. Data Sets

[19] The data sets that were used to test this model encompassed a wide range of canopy types: dowels simulating rigid submerged vegetation to plastic aquarium plants to real plants. The data sets were divided into rigid (53 data sets) and flexible vegetation (77 data sets). A brief explanation of the data sets and the related experimental conditions is given in Appendix B and Table 1. It must be emphasized here that the flexible vegetation in Table 1 is simply treated as rigid with  $h_c$  set as the reported bending height in the experiments. Hence, the interaction between the bulk flow and bending is not considered and is outside the scope of the present work given the need to model vegetation rigidity and the differential bending with the local velocity. While  $C_d$  varies with  $\bar{U}$ , and in some experiments listed in Table 1,  $a$  varies with  $z$ , we assumed throughout that  $C_d a$  does not vary appreciably with  $z$ . Some rationale for this approximation is that  $C_d$  tends to decrease with increasing  $z$  because of increased  $\bar{U}$ , while  $a$  is often larger in the mid to upper canopy when compared to the lower canopy for a number of aquatic (and terrestrial) vegetation. A height-independent  $C_d a$  is unrealistic in several regions of the canopy domain, including near the ground, which sets the lower-boundary condition. However, this assumption must be viewed within the scope of the primary objective here, which is not to model precisely all aspects of the vertical structure of the mean velocity profile but to provide roughness estimates as a function of two dimensionless groups. As noted in Table 1, the “intra” variation of  $C_d a$  across experiments by far exceeds the vertical (or “inter”) variation in  $C_d a$  for any one experiment.

[20] Currently, canopy lidar measurements can provide estimates of total leaf area index and canopy height so that  $a \approx LAI/h$  is the available bulk quantity from remote sensing. In the case of forested canopies, the vertical dimension of the canopy is sufficiently large (of order 10 m) so that canopy lidar can also provide a detailed profile of  $a$  [Lefsky *et al.*, 2002]. Aquatic vegetations are much shorter ( $< 1$  m), and detailed profiles of the vertical structure of  $a$  remain difficult to obtain. General expressions for  $C_d$  that account for sheltering effects are also absent and remain the subject of

**Table 1.** Summary of the Data Sets Used in Model Evaluation<sup>a</sup>

	Experiment Number	Q (m <sup>3</sup> s <sup>-1</sup> )	H <sub>w</sub> (m)	h <sub>c</sub> (m)	Slope	a (m <sup>-1</sup> )	Density (m <sup>-2</sup> )	C <sub>d</sub>
		<i>Rigid Canopies</i>						
<i>Lopez and Garcia</i> [2001] <sup>b</sup>	LG-1	0.179	0.335	0.12	0.0036	1.09	170	1.13
	LG-2	0.088	0.229	0.12	0.0036	1.09	170	1.13
	LG-3	0.046	0.164	0.12	0.0036	1.09	170	1.13
	LG-4	0.178	0.276	0.12	0.0076	1.09	170	1.13
	LG-5	0.098	0.203	0.12	0.0076	1.09	170	1.13
	LG-6	0.178	0.267	0.12	0.0036	0.27	42	1.13
	LG-7	0.095	0.183	0.12	0.0036	0.27	42	1.13
	LG-8	0.180	0.391	0.12	0.0036	2.46	384	1.13
	LG-9	0.058	0.214	0.12	0.0036	2.46	384	1.13
	LG-10	0.180	0.265	0.12	0.0161	2.46	384	1.13
	LG-11	0.177	0.311	0.12	0.0036	0.62	97	1.13
	LG-12	0.181	0.233	0.12	0.0110	0.62	97	1.13
<i>Poggi et al.</i> [2004c] <sup>c</sup>	P-D1	0.162	0.6	0.12	0.00004	0.27	67	1.00
	P-D2	0.162	0.6	0.12	0.00007	0.54	134	1.00
	P-D3	0.162	0.6	0.12	0.00011	1.07	268	1.00
	P-D4	0.162	0.6	0.12	0.00018	2.14	536	1.15
	P-D5	0.162	0.6	0.12	0.00032	4.29	1072	1.25
<i>Meijer and Van Velzen</i> [1999] <sup>d</sup>	MV-T22	3.557	2.08	0.9	0.00138	2.05	256	0.97
<i>Ghisalberti and Nepf</i> [2004] <sup>e</sup>	GN-A	4.80E-03	0.467	0.139	0.0000099	2.50	391	1.20
	GN-B	1.70E-03	0.467	0.139	0.0000018	2.50	391	1.40
	GN-C	7.40E-03	0.467	0.139	0.0000250	3.40	531	1.10
	GN-D	4.80E-03	0.467	0.139	0.0000120	3.40	531	1.10
	GN-E	1.43E-02	0.467	0.138	0.0000750	4.00	625	0.95
	GN-F	9.40E-03	0.467	0.138	0.0000320	4.00	625	0.99
	GN-G	4.80E-03	0.467	0.138	0.0000130	4.00	625	1.10
	GN-H	1.43E-02	0.467	0.138	0.0001000	8.00	1250	0.79
	GN-I	9.40E-03	0.467	0.138	0.0000340	8.00	1250	0.84
	GN-J	4.80E-03	0.467	0.138	0.0000130	8.00	1250	0.92
	GN-K	1.70E-03	0.467	0.138	0.0000026	8.00	1250	1.10
<i>Murphy et al.</i> [2007] <sup>f</sup>	MGN-A	4.80E-03	0.467	0.14	0.0000099	2.50	417	1.00
	MGN-C	7.40E-03	0.467	0.14	0.0000250	3.40	567	1.00
	MGN-D	4.80E-03	0.467	0.14	0.0000120	3.40	567	1.00
	MGN-E	1.43E-02	0.467	0.14	0.0000750	4.00	667	1.00
	MGN-G	4.80E-03	0.467	0.14	0.0000130	4.00	667	1.00
	MGN-H	1.43E-02	0.467	0.14	0.0001000	8.00	1333	1.00
	MGN-I	9.40E-03	0.467	0.14	0.0000340	8.00	1333	1.00
	MGN-A6	1.70E-03	0.298	0.07	0.0000030	2.50	417	1.00
	MGN-B6	9.40E-03	0.298	0.07	0.0000804	2.50	417	1.00
	MGN-C6	4.80E-03	0.298	0.07	0.0000242	2.50	417	1.00
	MGN-A1	1.70E-03	0.236	0.07	0.0000106	2.50	417	1.00
	MGN-B1	9.40E-03	0.236	0.07	0.0001157	2.50	417	1.00
	MGN-C1	4.80E-03	0.236	0.07	0.0000427	2.50	417	1.00
	MGN-A2	1.70E-03	0.14	0.07	0.0000173	2.50	417	1.00
	MGN-B2	9.40E-03	0.14	0.07	0.0004866	2.50	417	1.00
	MGN-C2	4.80E-03	0.14	0.07	0.0003005	2.50	417	1.00
	MGN-A3	1.70E-03	0.105	0.07	0.0001244	2.50	417	1.00
	MGN-C3	4.80E-03	0.105	0.07	0.0006661	2.50	417	1.00
	MGN-A5	1.70E-03	0.088	0.07	0.0002835	2.50	417	1.00
	MGN-C5	4.80E-03	0.088	0.07	0.0013404	2.50	417	1.00
	MGN-C6D	4.80E-03	0.298	0.07	0.0000203	8.00	1333	1.00
	MGN-C2D	4.80E-03	0.14	0.07	0.0003664	8.00	1333	1.00
	MGN-A2D	1.70E-03	0.14	0.07	0.0000474	8.00	1333	1.00
	MGN-A3D	1.70E-03	0.105	0.07	0.0002319	8.00	1333	1.00
		<i>Flexible Canopies; h<sub>c</sub> Is Undelected Height</i>						
<i>Baptist</i> [2003] <sup>g</sup>	B-2	0.133	0.306	0.18	0.005	2.00	400	1.00
	B-3	0.101	0.287	0.18	0.005	2.00	400	1.10
<i>Meijer and Van Velzen</i> [1999] <sup>h</sup>	MV-R6	1.313	1.99	1.58	0.00191	1.46	256	1.80
<i>Nepf and Vivoni</i> [2000] <sup>i</sup>	NV-2.75	0.015	0.44	0.16	0.0002	5.00	330	1.20
<i>Shi et al.</i> [1995] <sup>j</sup>	S-100	0.0053	0.348	0.3	0.00060	1.40	350	1.00
	S-80	0.0051	0.346	0.24	0.00060	1.40	350	1.00
	S-60	0.0028	0.338	0.18	0.00007	1.40	350	1.00
	S-40	0.0039	0.342	0.12	0.00003	1.40	350	1.00
	S-20	0.0033	0.332	0.06	0.00003	1.40	350	1.00
		<i>Flexible Canopies; h<sub>c</sub> Is Deflected Height</i>						
<i>Jarvela</i> [2005] <sup>k</sup>	J-R4-1	0.040	0.3060	0.205	0.0015	33.60	12000	1.25
	J-R4-2	0.100	0.3084	0.155	0.0036	33.60	12000	1.25
	J-R4-3	0.040	0.4065	0.230	0.0005	33.60	12000	1.25
	J-R4-4	0.100	0.4041	0.190	0.0013	33.60	12000	1.25
	J-R4-5	0.143	0.4070	0.160	0.0020	33.60	12000	1.25
	J-R4-6	0.040	0.5044	0.245	0.0002	33.60	12000	1.25
	J-R4-7	0.100	0.4950	0.220	0.0006	33.60	12000	1.25
	J-R4-8	0.100	0.7065	0.260	0.0002	33.60	12000	1.25

**Table 1.** (continued)

	Experiment Number	Q (m <sup>3</sup> s <sup>-1</sup> )	H <sub>w</sub> (m)	h <sub>c</sub> (m)	Slope	a (m <sup>-1</sup> )	Density (m <sup>-2</sup> )	C <sub>d</sub>
<i>Carollo et al.</i> [2002] <sup>l</sup>	J-R4-9	0.143	0.7037	0.215	0.0003	33.60	12000	1.25
	C-R1	0.0376	0.119	0.048	0.010	31.00	31000	1.10
	C-R2	0.0301	0.135	0.080	0.010	44.00	44000	1.10
	C-R3	0.0301	0.146	0.080	0.002	44.00	44000	1.10
	C-R4	0.0269	0.140	0.082	0.002	44.00	44000	1.10
	C-R5	0.0269	0.125	0.077	0.010	44.00	44000	1.10
	C-R6	0.0776	0.178	0.070	0.002	44.00	44000	1.10
	C-R7	0.0776	0.168	0.066	0.010	44.00	44000	1.10
	C-R8	0.1059	0.199	0.063	0.002	44.00	44000	1.10
	C-R9	0.1059	0.183	0.059	0.010	44.00	44000	1.10
	C-R10	0.0269	0.128	0.070	0.002	28.00	28000	1.10
	C-R11	0.0776	0.190	0.054	0.002	28.00	28000	1.10
	C-R12	0.1059	0.217	0.049	0.002	28.00	28000	1.10
	C-R13	0.1350	0.245	0.047	0.002	28.00	28000	1.10
	C-R14	0.1708	0.272	0.045	0.002	28.00	28000	1.10
	C-R15	0.1887	0.277	0.038	0.002	33.70	33700	1.10
C-R16	0.1892	0.272	0.031	0.002	33.70	33700	1.10	
<i>Ciralo and Ferreri</i> [2007] <sup>m</sup>	CF-R5	0.0574	0.150	0.068	0.00850	5.19	1037	2.00
	CF-R6	0.0681	0.161	0.063	0.00811	5.19	1037	2.00
	CF-R10	0.0750	0.249	0.105	0.00198	5.19	1037	2.00
	CF-R11	0.0951	0.243	0.095	0.00291	5.19	1037	2.00
	CF-R12	0.1099	0.245	0.100	0.00397	5.19	1037	2.00
	CF-R13	0.0270	0.360	0.235	0.00009	5.19	1037	2.00
	CF-R14	0.0550	0.367	0.160	0.00032	5.19	1037	2.00
	CF-R15	0.0840	0.365	0.140	0.00061	5.19	1037	2.00
	CF-R16	0.1161	0.348	0.118	0.00103	5.19	1037	2.00
	CF-R17	0.1346	0.350	0.115	0.00138	5.19	1037	2.00
	CF-R18	0.1574	0.348	0.105	0.00174	5.19	1037	2.00
	CF-R19	0.0349	0.466	0.290	0.00008	5.19	1037	2.00
	CF-R20	0.0689	0.470	0.190	0.00019	5.19	1037	2.00
	CF-R21	0.1081	0.478	0.235	0.00045	5.19	1037	2.00
CF-R22	0.1456	0.474	0.115	0.00055	5.19	1037	2.00	
CF-R23	0.1770	0.465	0.145	0.00081	5.19	1037	2.00	
	<i>Flexible Canopies; h<sub>c</sub> Is Deflected Height</i>							
<i>Kouwen and Unny</i> [1969] <sup>n</sup>	K-1	0.0027	0.1506	0.100	0.0005	25.00	5000	1.00
	K-2	0.0169	0.2527	0.100	0.0010	25.00	5000	1.00
	K-3	0.0856	0.3819	0.085	0.0030	25.00	5000	1.00
	K-4	0.0091	0.1519	0.100	0.0050	25.00	5000	1.00
	K-7	0.0132	0.1509	0.100	0.0100	25.00	5000	1.00
	K-8	0.0827	0.2422	0.050	0.0094	25.00	5000	1.00
	K-9	0.0437	0.3503	0.100	0.0010	25.00	5000	1.00
	K-10	0.0408	0.2500	0.100	0.0049	25.00	5000	1.00
	K-11	0.0381	0.4000	0.100	0.0005	25.00	5000	1.00
	K-12	0.0194	0.3000	0.100	0.0005	25.00	5000	1.00
	K-14	0.0067	0.2002	0.100	0.0005	25.00	5000	1.00
	K-15	0.0496	0.3000	0.095	0.0030	25.00	5000	1.00
	K-16	0.0097	0.2001	0.100	0.0010	25.00	5000	1.00
	K-17	0.0479	0.1990	0.060	0.0100	25.00	5000	1.00
	K-18	0.0284	0.3498	0.100	0.0005	25.00	5000	1.00
	K-19	0.0731	0.2998	0.075	0.0050	25.00	5000	1.00
	K-20	0.0288	0.3000	0.100	0.0010	25.00	5000	1.00
	K-21	0.0165	0.2000	0.100	0.0030	25.00	5000	1.00
K-22	0.0225	0.2000	0.100	0.0050	25.00	5000	1.00	
K-24	0.1139	0.3486	0.060	0.0050	25.00	5000	1.00	
K-25	0.0558	0.3986	0.090	0.0010	25.00	5000	1.00	
K-26	0.0127	0.2527	0.100	0.0005	25.00	5000	1.00	
K-27	0.0754	0.3508	0.090	0.0030	25.00	5000	1.00	
K-28	0.0310	0.2594	0.100	0.0030	25.00	5000	1.00	
K-29	0.1422	0.3830	0.055	0.0049	25.00	5000	1.00	
K-30	0.0038	0.1491	0.100	0.0010	25.00	5000	1.00	

**Table 2.** Comparisons Between Measured and Modeled Bulk Velocity  $U_b$  Using the Two Mixing Length Models for All Rigid and Flexible Canopies<sup>a</sup>

	Proposed Model	MV99
	<i>Rigid Canopy</i>	
$m$	0.95	1.06
$b$ (m s <sup>-1</sup> )	0.02	0.03
$R^2$	0.95	0.95
RMSE (m s <sup>-1</sup> )	0.05	0.07
	<i>Flexible Canopy</i>	
$m$	1.03	1.70
$b$ (m s <sup>-1</sup> )	0.09	0.07
$R^2$	0.57	0.59
RMSE (m s <sup>-1</sup> )	0.21	0.27

<sup>a</sup>The regression model is  $\hat{y} = m \hat{x} + b$ , where  $\hat{y}$  are measured and  $\hat{x}$  are modeled  $U_b$  (m s<sup>-1</sup>). The regression slope ( $m$ ) and intercept ( $b$ ), the coefficient of determination ( $R^2$ ), and the root-mean-square error (RMSE), are shown. The sample sizes for the rigid and flexible canopy cases are 57 and 73, respectively.

active research in both terrestrial and aquatic vegetation turbulence [Finnigan, 2000; Nepf, 1999; Nepf et al., 2007; Poggi et al., 2004c; Raupach, 1992, 1994]. Hence, remotely sensed field measurements remain unable to account for the depth variations of  $C_{da}$  though, as earlier stated, the formulations and closure schemes can account for them if they are available.

[21] By decomposing the analysis here into rigid (mainly rods) and flexible canopies, we can assess how robust the formulations are to a depth-independent  $C_{da}$  simplification. For the rod canopy type,  $a$  is generally constant but  $C_d$  varies with  $z$  because of depth variations in  $\bar{U}$ . However, in the case of flexible canopies, both  $C_d$  and  $a$  vary with  $z$  (up to factors of 2), though often exhibiting opposite vertical trends.

#### 4. Model Evaluation for $U_b$

[22] The model evaluation utilizes both mixing length approaches to compute profiles of  $\bar{U}$  and  $\overline{u'w'}$ . From these profiles,  $U_b = \frac{1}{H_w} \int_0^{H_w} U(z) dz$  is computed and compared with measured  $U_b$  (see<sup>d</sup> Table 2).

[23] Figure 2 provides a sample comparison between measured and modeled  $\bar{U}$  and  $\overline{u'w'}$  for three distinct vegetation types as defined in Table 1, again confirming a good agreement between measured and modeled  $\overline{u'w'}$  inside the canopy. The comparison between measured and mod-

eled  $\bar{U}$  inside the canopy appears consistent with the  $\overline{u'w'}$  comparisons; however, well above the canopy the agreement degrades. Several reasons for this degradation can be postulated, but two plausible ones include (1) the mixing length near the water surface is not adequately described by  $\tau_{eff}^s = k_v (z - d)$  [Poggi et al., 2004c] and (2)  $d\bar{U}/dz \neq 0$  as  $z \rightarrow H_w$  (as evidenced by some of the data sets in Table 1). Figure 3 explores whether these disagreements are significant enough to impact  $U_b$  predictions.

[24] Both mixing length models reproduced well (to within 5%, see regression slopes in Table 2) the measured  $U_b$  for rigid canopies as shown in Figure 3 despite the height-independent  $C_{da}$  simplification across experiments. However, the agreement between measurements and models degraded for flexible canopies and for both mixing length models (see the fourfold increase in root-mean-square error in Table 2 when comparing rigid with flexible), but more so for the MV99 model (see regression slopes in Table 2). As earlier stated, the assumption of depth-independent  $C_{da}$  is much more restrictive in flexible vegetation. Also, the drag reduction due to vegetation bending and its dependence on local velocity is not accounted for in these calculations, a topic that requires further exploration.

#### 5. Results

[25] Using the first-order closure model with the proposed mixing length (equation (15)),  $f$  was computed from  $U_b/u_*$  for a wide range of  $H_w/h_c$  and  $L_c/h_c$  values while keeping  $S$  constant at 1%. The computed  $f$ , shown in Figure 4, varies with both  $H_w/h_c$  and  $L_c/h_c$  in a nonlinear manner (even in a log-log representation). As expected,  $f$  decreases with increasing  $H_w/h_c$  for a given set of canopy attributes (i.e.,  $L_c/h_c$ ). Also, for a given submersion regime (i.e.,  $H_w/h_c$ ),  $f$  decreases with increasing  $L_c/h_c$ . To test whether these results are dependent on the choice of  $S$  (and hence  $U_b$ ), these model calculations were repeated for a wide range of  $S \in [0.05\% - 5\%]$  (and hence Reynolds number) and the results in Figure 4 remained unaltered with variations in  $S$ . Note that each of the five lines in Figure 4 is for three different Reynolds numbers. These findings suggest that modeled  $f$  does not depend on the Reynolds number when assuming  $L_c$  is independent of  $\bar{U}$ . To further assess whether these computed  $f$  agree with measurements, the data in Table 1 was clustered into groups of  $L_c/h_c$  and  $f$  was plotted as a function of  $H_w/h_c$  for each of these groups, as shown in Figure 4. Again, good agreement between modeled and

Notes to Table 1:

<sup>a</sup>The model input includes water level  $H_w$ , canopy height  $h_c$ , an estimate of the canopy density  $a$ , channel slope ( $S$ ), and the drag coefficient  $C_d$  (either reported or estimated). For some experiments,  $a$  was estimated from the stem density  $n_s$  and stem diameter  $d$  using  $a = n_s d$ . When the drag coefficient was not provided, it was either assumed to be unity (i.e., isolated cylinder) or in some cases, it was set to a value reported for similar vegetation and setup.

<sup>b</sup>Wooden dowels, steam diameter 0.0064, CW = 0.91 m.

<sup>c</sup>Steel cylinders, steam diameter 0.004 m, CW = 0.90 m.

<sup>d</sup>Steel bars, CW = 3.00 m.

<sup>e</sup>Wooden dowels, steam diameter 0.0064 m, CW = 0.38 m.

<sup>f</sup>Wooden dowels, steam diameter 0.006 m, CW = 0.38 m.

<sup>g</sup>Plastic aquarium plants, steam diameter 0.005 m, CW = 0.80 m.

<sup>h</sup>Natural reed, steam diameter 0.0057 m, CW = 3.00 m.

<sup>i</sup>Plastic plant prototype, CW = 0.38 m.

<sup>j</sup>*Spartina anglica* steam diameter, 0.004 m, CW = 0.30 m.

<sup>k</sup>Wheat stems, steam diameter 0.0028 m, CW = 1.10 m.

<sup>l</sup>Mixed grasses, steam diameter 0.001 m, CW = 0.60 m.

<sup>m</sup>*Posidonia oceanica* steam diameter, 0.005 m, CW = 0.77 m.

<sup>n</sup>Styrene strips, steam diameter 0.005 m, CW = 0.61 m.

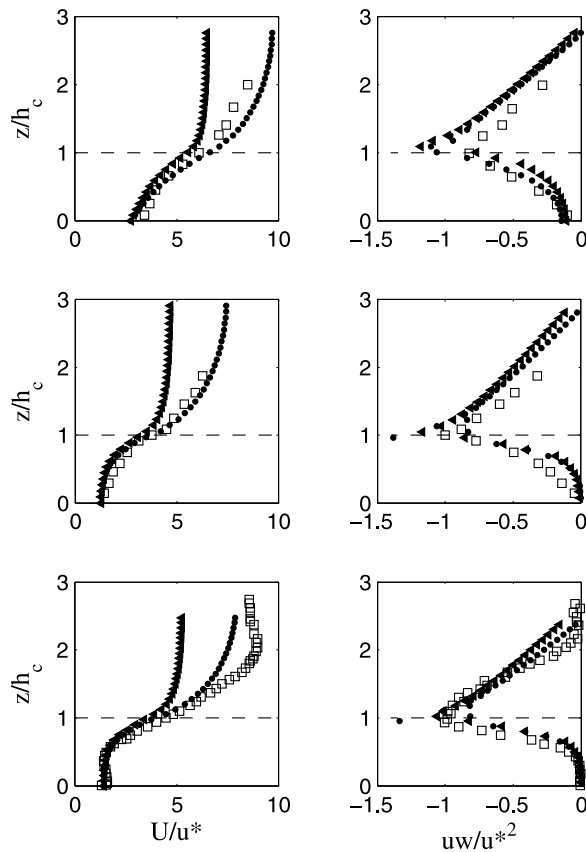


**Figure 2.** Comparison between measured and modeled (left) normalized mean velocity ( $U/u_*$ ) and (right) turbulent flux ( $\overline{uw}/u_*^2$ ) with normalized depth ( $z/h_c$ ), where  $u_*$  is the friction velocity and  $h_c$  is the canopy height. Shown are data from (top) Lopez and Garcia [2001] (LG1), (middle) Poggi et al. [2004c] (P-D5), and (bottom) Nepf and Vivoni [2000] (NV-2.75). The flow conditions for each experiment are presented in Table 1. Circles are for the proposed mixing length model, and triangles are from MV99 (equation (14)).

measured  $f$  was noted in Figure 4 given the “heterogeneity” in the collected data (which includes the 73 flexible vegetation runs).

[26] The fact that  $f$  appears insensitive to the bulk Reynolds number has implications on the so-called “retardance curves,” routinely used in hydraulics designs. Guidelines for the hydraulic design of vegetated channels using the retardance curves for erosion control are reviewed elsewhere [Chow, 1959]. The classical retardance curves of Chow [1959] present  $n$  as a function of  $U_b H_w$ , for flexible vegetation, clustering them on the basis of their rigidity index. Figure 5 presents the model results in Figure 4 (for rigid vegetation) after computing  $n$  from  $f$  using different  $h_c$  ( $= 10$  cm,  $20$  cm, and  $40$  cm) but keeping  $S = 1\%$ . As expected, the Reynolds number fails to collapse these data thereby confirming that  $H_w/h_c$  remains the leading variable describing the bulk resistance factor at a constant  $L_c/h_c$  (i.e., when canopy attributes are constant). We should note that recent flume experiments are suggestive that  $f$  is more sensitive to flow depth in the case of rigid vegetation when compared to its flexible counterpart [Musleh and Cruise, 2006], as expected. Notwithstanding this differential sensitivity, the spread in the model results here for rigid

canopies is commensurate with the reported spread of the retardance curves by Chow [1959], also repeated in Figure 5 for reference. It is clear that isolating the effects of relative submergence from other factors, including Reynolds number, remains a crucial point for models of  $f$  or  $n$  whether be it for rigid or flexible vegetation.

## 6. Discussion and Conclusion

[27] Recent developments in remote sensing technologies are now permitting an unprecedented view of water level variations, canopy height, and leaf area distribution at large spatial scales. These developments are now renewing interest in effective resistance formulations for vegetated surfaces that preserve the nonlinearities in the functional relationship between the resistance value, the canopy attributes, and water depth. Using a simplified scaling analysis on the depth-integrated mean momentum balance, the friction factor  $f$  was shown to be dominated by three length scales: the water depth  $H_w$ , the canopy height  $h_c$ , and the adjustment length scale  $L_c = (C_d a)^{-1}$ . These length scales form two dimensionless groups: the submergence depth ( $H_w/h_c$ ) and the adjustment length to canopy height ratio ( $L_c/h_c$ ). The dependence of  $f$  on these two functional groups was then

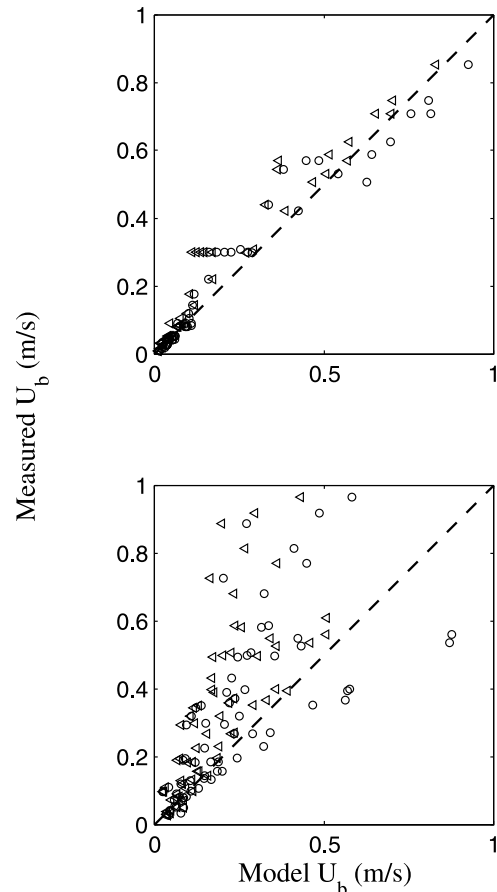


**Figure 3.** Comparison between measured and modeled bulk velocity ( $U_b$ ) for (top) rigid and (bottom) flexible vegetation. The 1:1 line is shown. Circles are the proposed model and triangles are from the MV99 mixing length model. For flexible vegetation, the data set well above the 1:1 line is mainly from Carollo et al. [2002].

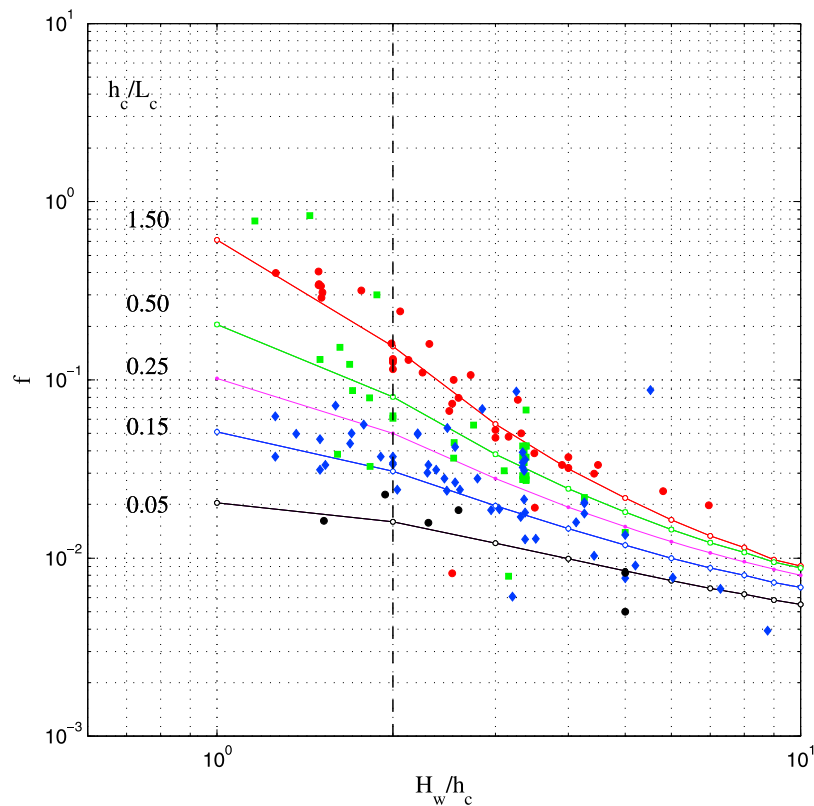


**Figure 4.** Variations of the friction factor  $f$  with submergence depth ( $H_w/h_s$ ) for various  $h_c/L_c$ . The model calculations are shown by solid lines, and all the data in Table 1 are shown by symbols. Each line is for three different Reynolds numbers. The color of the symbols represents the following thresholds of  $h_c/L_c$ : black  $<0.1$ , blue  $0.1-0.4$ , green  $0.4-1.4$ , and red  $>1.4$ .

explored using a combination of first-order closure modeling and 130 published runs from flume experiments for rigid (57 runs) and flexible (73 runs) vegetation. Preliminarily, the first-order closure model was evaluated using these data sets and was shown to reproduce the bulk velocity to within 5% for rigid canopies. When flexible canopies were treated as rigid canopies with a constant deflected height, the model was also shown to reproduce the bulk velocity reasonably well though the root-mean-square error was fourfold higher when compared to the rigid case.

[28] The experimental data sets and the first-order closure model was then used to explore the relationship between  $f$  and the two dimensionless groups for a wide range of  $H_w/h_c$  and  $L_c/h_c$ . Both the data and the results from the model show a nonlinear decrease in  $f$  with increasing  $H_w/h_c$  at a given  $L_c/h_c$  and the nonlinear increase in  $f$  with decreasing  $L_c/h_c$ . Furthermore, the results did not exhibit any dependence on the bulk Reynolds number. Good agreement between the experimental data and the numerical results was noted.

[29] These findings have practical applications for a number of design problems. For example, the design of swale (or lined grass channel) installations for urban pollution control require  $H_w/h_c \sim 1$ , contrary to swale design for erosion control [Kirby *et al.*, 2005]. For such design conditions, the model results qualitatively agree with recent small-flume experiments that documented significant reduction in hydraulic resistance when the flow depth was increased

[Kirby *et al.*, 2005] though the model here does not attribute this reduction to an increase in bulk Reynolds number. Another application is the construction or restoration of degraded wetlands. Much of these designs also rely on retardance curves [Tsihrintzis and Madiedo, 2000] that do not explicitly consider  $H_w/h_c$ .

[30] While these model-data comparisons for bulk velocity are encouraging, a number of “thorny” issues remain to be confronted. First, the analysis here focused on rigid canopies, and flexible canopies were simply treated as rigid vegetation with modified canopy height a priori set to the bending height. Hence, the model calculations exclude any possible interactions between the bulk flow and vegetation bending, a topic that is receiving significant attention. Second, the closure model primarily dealt with submerged canopies, though the flow through emergent canopies may play a crucial role in the hydrologic description of basin flooding and its recession. Third, the formulations here did not consider the role of complex topography, also known to impact the bulk flow properties. This is a topic that is gaining significant attention in terrestrial ecosystems in the context of drainage flow of  $\text{CO}_2$  and estimating nighttime respiration from eddy covariance data. Fourth, wind effects are completely neglected, and while there is a wealth of studies on wind-water interactions, the findings from such studies have not been tested for flexible emergent canopies, where wind effects may play a prominent role in bending the vegetation. Progress on all these topics must take advan-

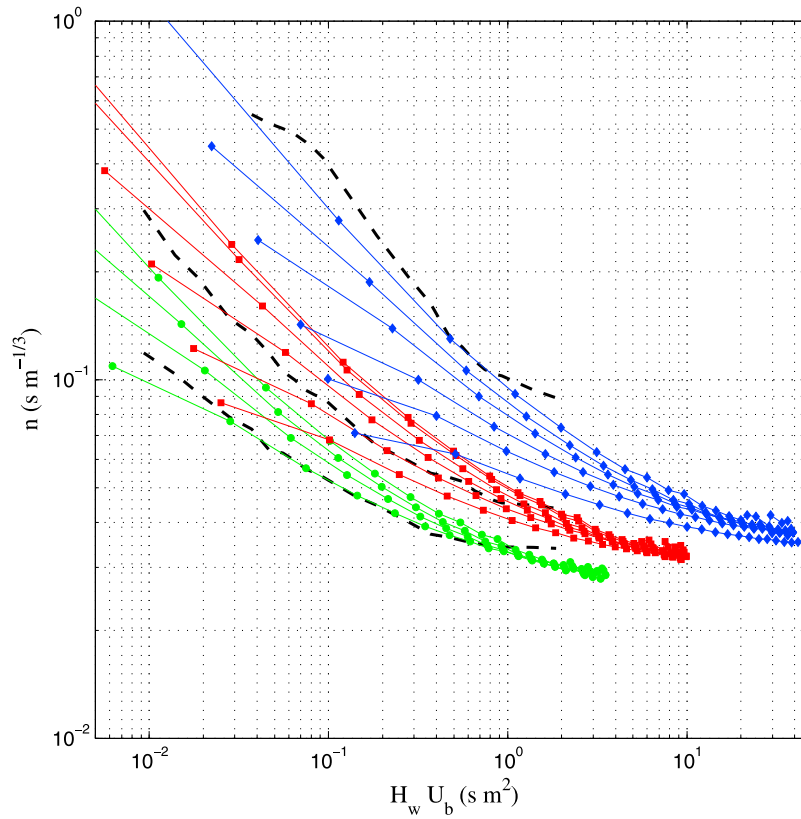


**Figure 5.** Variations of Manning's roughness ( $n$ ) as a function of the bulk Reynolds number ( $U_b H_w$ ) for the same results shown in Figure 4. Note that the bulk Reynolds number fails to collapse the model results. For reference, typical retardance curves from *Chow* [1959] are also shown.

tage of all possible venues, including novel flume and field experiments, large eddy simulations, and simplified scaling analysis.

## Appendix A

[31] The mixing length proposed in section 2.2 primarily holds for dense canopies [*Poggi et al.*, 2004b, 2004c; *Poggi and Katul*, 2007b]. To estimate how dense the canopy needs to be for the model to be valid, consider the within-canopy eddy decorrelation or relaxation time scale, given by

$$\tau_e = \frac{k}{\varepsilon_{isr} + W_D}, \quad (\text{A1})$$

where  $\varepsilon_{isr}$  is the TKE dissipation rate for an inertial energy cascade unaltered by the presence of the canopy, and  $W_D \approx C_d a \bar{U} k$  is the work done by turbulence to overcome the canopy drag and produce wakes. Inside dense canopies [*Finnigan*, 2000],

$$\varepsilon_{isr} \ll W_D$$

resulting in

$$\tau_e = \frac{k}{W_D} \approx \frac{1}{C_d a \bar{U}}. \quad (\text{A2})$$

Using Taylor's frozen turbulence hypothesis, the adjustment length scale [*Belcher et al.*, 2003; *Finnigan*, 2000; *Nepf et al.*, 2007] now emerges when defined as  $L_c = \tau \bar{U}$ , to yield

$$L_c = \frac{1}{C_d a}. \quad (\text{A3})$$

Hence the adjustment length scale measures how quickly the turbulent kinetic energy in eddies advecting at  $\bar{U}$  are dissipated by their work to overcome the drag elements. This length scale can be compared to the shear length scale produced by the inflection point instability near the canopy top, defined as [*Finnigan*, 2000; *Raupach et al.*, 1996]

$$L_s = \frac{\bar{U}}{\partial \bar{U} / \partial z}. \quad (\text{A4})$$

For a near-exponential mean velocity profile attenuated at a rate  $\beta = \frac{u_*}{\bar{U}}$  within dense canopies,  $L_s = h_c / \beta$ , resulting in  $L_s L_c \approx h_c / \beta C_d a \approx C_d a h_c \bar{U} / u_*$ .

[32] If  $L_s / L_c = 1$ , then eddies produced by inflectional instabilities in the mean velocity profile near the canopy top will be entirely dissipated by the foliage drag within one adjustment length. Hence, a possible quantification of "dense" vegetation, using one of the dimensionless groups earlier shown to control  $f$ , can be formulated as

$$\frac{h_c}{L_c} = C_d a h_c \geq \frac{\bar{U}}{u_*} \Big|_{z=h_c}. \quad (\text{A5})$$

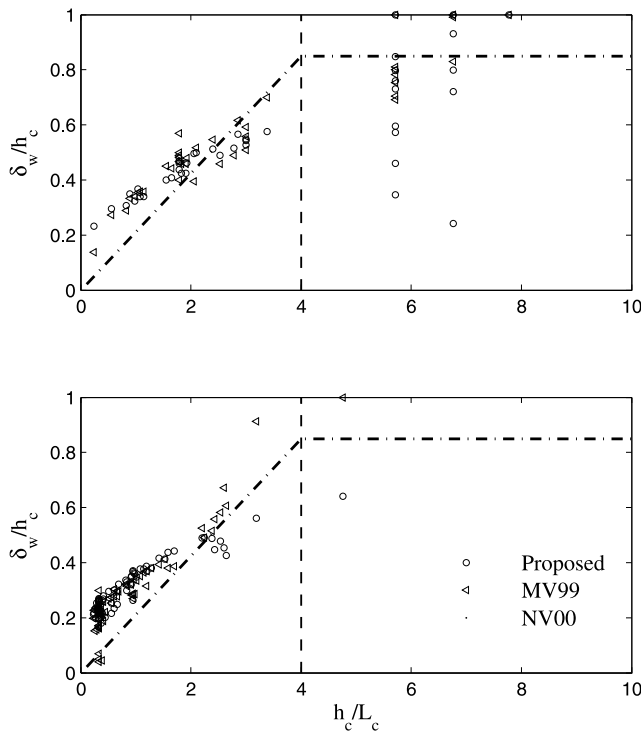


**Figure 6.** Variations of the normalized penetration depth ( $\delta_w/h_c$ ) with  $h_c/L_c$  for (top) rigid and (bottom) flexible canopies. The threshold reported by *Nepf and Vivoni* [2000] (NV00) is shown as a vertical dashed line. Dense canopies are defined as  $h_c/L_c > 4$ .

For dense canopies within terrestrial ecosystems,  $\bar{U}/u_*|_{z=h_c} \approx 3.33$  [*Katul et al.*, 1998; *Massman*, 1997; *Raupach et al.*, 1996], and  $C_d a h_c \geq 3.33$ . This limit is not significantly different from  $C_d a h_c \geq 4$  empirically derived by *Nepf and Vivoni* [2000] for aquatic vegetation though this limit may vary with the precise distribution of roughness elements [*Jimenez*, 2004]. Using published data from a wide range of experiments, *Nepf and Vivoni* [2000] found that the value of  $L_c/h_c$  when  $\delta_w$  became independent from  $h_c/L_c$  was around 4. In terrestrial ecosystems,  $a$  can be estimated from  $a = LAI/h_c$ , where LAI is the leaf area index (that can be measured via remote sensing products) and  $C_d \in [0.15-0.3]$ . It is clear that for terrestrial ecosystems, when  $LAI > 3$ , the canopy may be treated as dense as is often the case in practice [*Katul et al.*, 2004].

[33] Because the model computes the  $\overline{u'w'}$  profiles, predicted  $\delta_w$  variations with  $h_c/L_c$  can be compared with reported literature trends. In particular, data sets collected in aquatic and terrestrial vegetation suggest a best fit model to the ensemble  $\delta_w$  given by [*Nepf et al.*, 2007]

$$\frac{\delta_w}{h} = \begin{cases} 0.21 L_c/h_c, & \text{for } C_d a h_c > 4 \\ 0.85 - 1.0, & \text{otherwise} \end{cases} \quad (\text{A6})$$

Good agreement between predicted  $\delta_w$  from both mixing length models and estimated  $\delta_w$  from *Nepf et al.* [2007] is shown in Figure 6, suggesting that the attenuation profile of  $\overline{u'w'}$  is reasonably well reproduced for both canopy types. Again, the transition limit of about 4 reported by *Nepf et al.* [2007] is also reasonable given that the scaling length argu-

ment ( $L_s/L_c$ ) here is implicitly accounted for in the closure model.

## Appendix B

[34] For rigid canopies, twelve data sets described by *Lopez and Garcia* [2001], five data sets described by *Poggi et al.* [2004c], one data set from *Meijer and Van Velzen* [1999] eleven data sets from *Ghisalberti and Nepf* [2004] and 24 data sets from *Murphy et al.* [2007] were used. The flume experiments run by *Lopez and Garcia* comprised 12-cm tall cylindrical wooden dowels with a diameter of 6.4 mm. The five flume experiments from *Poggi et al.* were run using 12-cm tall stainless steel cylinders with a diameter of 4 mm. The rigid vegetation data set from *Meijer and Van Velzen* were steel bars, 8 mm in diameter and 90 cm tall. The eleven experiments from *Ghisalberti and Nepf* were run using wooden cylinders, 0.64 cm in diameter and 13.9 cm high. The 24 data sets were conducted using maple cylinders, 6 mm in diameter and 14 cm tall [*Murphy et al.*, 2007]. Note that some of the 24 runs of *Murphy et al.* [2007] duplicate those of *Ghisalberti and Nepf* [2004]. Not all 24 runs of *Murphy et al.* have been used in the following analysis.

[35] The flexible vegetation data sets were also obtained from a variety of experiments [*Baptist*, 2003; *Carollo et al.*, 2002; *Ciraolo and Ferreri*, 2007; *Jarvela*, 2005; *Kouwen and Unny*, 1969; *Meijer and Van Velzen*, 1999; *Nepf and Vivoni*, 2000; *Shi et al.*, 1995]. *Baptist* used plastic aquarium plants, AQUASCAPERS, from Metaframe Corporation, USA, type Anacharis (*Egeria densa*) X-large. *Meijer and Van Velzen* conducted their experiments using natural reeds, approximately 1.58 m high and 5.7 mm in diameter. Approximately half of the reeds had tufts growing from them with an average of two leaves. *Nepf and Vivoni* used a plastic plant prototype made of 0.025-cm thick vinyl plastic. Each plant had six 0.3-cm wide blades, bundled together to create a 2-cm high stem. The experiments by *Shi et al.* were run using *spartina anglica*, or cordgrass, collected from Humber Estuary in the United Kingdom. The average diameter of this vegetation was 4 mm, and all plants were chopped to 300 mm, the average height of plants measured in the field. *Jarvela's* experiments were conducted using wheat with a flexibility index similar to that of grass. The wheat stems were approximately 280 mm high and 2.8 mm in diameter. *Carollo* used a mixture of various grasses comprising approximately 50% *Loiatio*, 40% *Festuca rubra*, and 10% *Poa pratensis*. The stem diameter for this grass mixture was assumed by us to be 1 mm, which is an average for this type of grass. *Ciraolo and Ferrari* used an artificial canopy designed after the *Posidonia oceanica* plant, native to the Mediterranean Sea. The artificial canopy was modeled using low-density polyethylene strips. *Kouwen's* experiments were done using artificial flexible roughness element strips cut from 0.03-cm thick sheets of styrene. Table 1 summarizes all the data sets used here along with inputs and parameters needed for the closure model calculations.

[36] **Acknowledgments.** This research was supported, in part, by the National Science Foundation (NSF-EAR 06-35787 and NSF-EAR-06-28432).

## References

- Alsldorf, D. E., and D. P. Lettenmaier (2003), Tracking fresh water from space, *Science*, 301(5639), 1491–1494, doi:10.1126/science.1089802.
- Alsldorf, D. E., J. M. Melack, T. Dunne, L. A. K. Mertes, L. L. Hess, and L. C. Smith (2000), Interferometric radar measurements of water level changes on the Amazon flood plain, *Nature*, 404(6774), 174–177, doi:10.1038/35004560.
- Alsldorf, D., D. Lettenmaier, and C. Vorosmarty (2003), The need for global satellite based observations of terrestrial surface waters, *Eos Trans. AGU*, 84(29), 269, doi:10.1029/2003EO290001.
- Alsldorf, D., T. Dunne, J. Melack, L. Smith, and L. Hess (2005), Diffusion modeling of recessional flow on central Amazonian floodplains, *Geophys. Res. Lett.*, 32, L21405, doi:10.1029/2005GL024412.
- Alsldorf, D., P. Bates, J. Melack, M. Wilson, and T. Dunne (2007a), Spatial and temporal complexity of the Amazon flood measured from space, *Geophys. Res. Lett.*, 34, L08402, doi:10.1029/2007GL029447.
- Alsldorf, D. E., E. Rodriguez, and D. P. Lettenmaier (2007b), Measuring surface water from space, *Rev. Geophys.*, 45, RG2002, doi:10.1029/2006RG000197.
- Baptist, M. J. (2003), A flume experiment on sediment transport with flexible and submerged vegetation, paper presented at International Workshop on Riparian Forest Vegetated Channels: Hydraulic, Morphological and Ecological Aspects, Int. Assoc. for Hydraul. Res., Trento, Italy.
- Baptist, M. J., V. Babovic, J. R. Uthurburu, M. Keijzer, R. E. Uittenbogaard, A. Mynett, and A. Verwey (2007), On inducing equations for vegetation resistance, *J. Hydraul. Res.*, 45(4), 435–450.
- Belcher, S. E., N. Jerram, and J. C. R. Hunt (2003), Adjustment of a turbulent boundary layer to a canopy of roughness elements, *J. Fluid Mech.*, 488, 369–398, doi:10.1017/S0022112003005019.
- Carollo, F. G., V. Ferro, and D. Termini (2002), Flow velocity measurements in vegetated channels, *J. Hydraul. Eng.*, 128(7), 664–673, doi:10.1061/(ASCE)0733-9429(2002)128:7(664).
- Cheng, H., and I. P. Castro (2002), Near wall flow over urban-like roughness, *Boundary Layer Meteorol.*, 104(2), 229–259, doi:10.1023/A:1016060103448.
- Chow, V. T. (1959), *Open-Channel Hydraulics*, McGraw-Hill, New York.
- Ciraolo, G., and G. B. Ferreri (2007), Log velocity profile and bottom displacement for a flow over a very flexible submerged canopy, paper presented at 32nd Congress: Harmonizing the Demands of Art and Nature in Hydraulics, Int. Assoc. of Hydraul. Eng. and Res., Venice, Italy.
- Defina, A., and A. C. Bixio (2005), Mean flow and turbulence in vegetated open channel flow, *Water Resour. Res.*, 41, W07006, doi:10.1029/2004WR003475.
- Finnigan, J. (2000), Turbulence in plant canopies, *Annu. Rev. Fluid Mech.*, 32, 519–571, doi:10.1146/annurev.fluid.32.1.519.
- Finnigan, J. J., and S. E. Belcher (2004), Flow over a hill covered with a plant canopy, *Q. J. R. Meteorol. Soc.*, 130(596), 1–29, doi:10.1256/qj.02.177.
- Ghisalberti, M., and H. M. Nepf (2004), The limited growth of vegetated shear layers, *Water Resour. Res.*, 40, W07502, doi:10.1029/2003WR002776.
- Green, J. C. (2005), Modelling flow resistance in vegetated streams: review and development of new theory, *Hydrol. Processes*, 19, 1245–1259, doi:10.1002/hyp.5564.
- Helmert, M. J., and D. E. Eisenhauer (2006), Overland flow modeling in a vegetative filter considering non-planar topography and spatial variability of soil hydraulic properties and vegetation density, *J. Hydrol.*, 328(1–2), 267–282, doi:10.1016/j.jhydrol.2005.12.026.
- Helmio, T. (2002), Unsteady 1D flow model of compound channel with vegetated floodplains, *J. Hydrol.*, 269(1–2), 89–99, doi:10.1016/S0022-1694(02)00197-X.
- Huthoff, F., D. C. M. Augustijn, and S. J. M. H. Hulscher (2007), Analytical solution of the depth-averaged flow velocity in case of submerged rigid cylindrical vegetation, *Water Resour. Res.*, 43, W06413, doi:10.1029/2006WR005625.
- Jackson, P. S. (1981), On the displacement height in the logarithmic velocity profile, *J. Fluid Mech.*, 111, 15–25, doi:10.1017/S0022112081002279.
- Jarvela, J. (2002), Flow resistance of flexible and stiff vegetation: A flume study with natural plants, *J. Hydrol.*, 269(1–2), 44–54, doi:10.1016/S0022-1694(02)00193-2.
- Jarvela, J. (2005), Effect of submerged flexible vegetation on flow structure and resistance, *J. Hydrol.*, 307(1–4), 233–241, doi:10.1016/j.jhydrol.2004.10.013.
- Jimenez, J. (2004), Turbulent flows over rough walls, *Annu. Rev. Fluid Mech.*, 36, 173–196, doi:10.1146/annurev.fluid.36.050802.122103.
- Katul, G. G., C. D. Geron, C. I. Hsieh, B. Vidakovic, and A. B. Guenther (1998), Active turbulence and scalar transport near the forest-atmosphere interface, *J. Appl. Meteorol.*, 37(12), 1533–1546, doi:10.1175/1520-0450(1998)037<1533:ATASTN>2.0.CO;2.
- Katul, G. G., L. Mahrt, D. Poggi, and C. Sanz (2004), One- and two-equation models for canopy turbulence, *Boundary Layer Meteorol.*, 113(1), 81–109, doi:10.1023/B:BOUN.0000037333.48760.e5.
- Kirby, J. T., R. Durrans, R. Pitt, and P. D. Johnson (2005), Hydraulic resistance in grass swales designed for small flow conveyance, *J. Hydraul. Eng.*, 131(1), 65–68, doi:10.1061/(ASCE)0733-9429(2005)131:1(65).
- Kouwen, N., and T. E. Unny (1969), Flow retardance in vegetated channels, *J. Irrig. Drain. Div. Am. Soc. Civ. Eng.*, 95(IR2), 329–342.
- Lefsky, M. A., W. B. Cohen, G. G. Parker, and D. J. Harding (2002), Lidar remote sensing for ecosystem studies, *BioScience*, 52(1), 19–30, doi:10.1641/0006-3568(2002)052[0019:LRSFES]2.0.CO;2.
- Lopez, F., and M. H. Garcia (2001), Mean flow and turbulence structure of open-channel flow through non-emergent vegetation, *J. Hydraul. Eng.*, 127(5), 392–402, doi:10.1061/(ASCE)0733-9429(2001)127:5(392).
- Massman, W. J. (1997), An analytical one-dimensional model of momentum transfer by vegetation of arbitrary structure, *Boundary Layer Meteorol.*, 83(3), 407–421, doi:10.1023/A:1000234813011.
- Meijer, D. G., and E. H. Van Velzen (1999), Prototype scale flume experiments on hydraulic roughness of submerged vegetation, paper presented at 28th International Conference, Int. Assoc. of Hydraul. Eng. and Res., Graz, Austria.
- Murphy, E., M. Ghisalberti, and H. Nepf (2007), Model and laboratory study of dispersion in flows with submerged vegetation, *Water Resour. Res.*, 43, W05438, doi:10.1029/2006WR005229.
- Musleh, F. A., and J. F. Cruise (2006), Functional relationships of resistance in wide flood plains with rigid unsubmerged vegetation, *J. Hydraul. Eng.*, 132(2), 163–171, doi:10.1061/(ASCE)0733-9429(2006)132:2(163).
- Neary, V. S. (2003), Numerical solution of fully developed flow with vegetative resistance, *J. Eng. Mech.*, 129(5), 558–563, doi:10.1061/(ASCE)0733-9399(2003)129:5(558).
- Nepf, H. M. (1999), Drag, turbulence, and diffusion in flow through emergent vegetation, *Water Resour. Res.*, 35(2), 479–489, doi:10.1029/1998WR900069.
- Nepf, H. M., and E. R. Vivoni (2000), Flow structure in depth-limited, vegetated flow, *J. Geophys. Res.*, 105(C12), 28,547–28,557, doi:10.1029/2000JC900145.
- Nepf, H. M., B. L. White, A. F. Lightbody, and M. Ghisalberti (2007), Transport in aquatic canopies, in *Flow and Transport Processes With Complex Obstructions: Applications to Cities, Vegetative Canopies, and Industry*, NATO Sci. Ser. II, vol. 236, edited by Y. A. Gayev and J. C. R. Hunt, pp. 221–250, Springer, Berlin.
- Nikora, V., D. Goring, I. McEwan, and G. Griffiths (2001), Spatially averaged open-channel flow over rough bed, *J. Hydraul. Eng.*, 127(2), 123–133, doi:10.1061/(ASCE)0733-9429(2001)127:2(123).
- Nikora, V., K. Koll, I. McEwan, S. McLean, and A. Dittrich (2004), Velocity distribution in the roughness layer of rough-bed flows, *J. Hydraul. Eng.*, 130(10), 1036–1042, doi:10.1061/(ASCE)0733-9429(2004)130:10(1036).
- Poggi, D., and G. Katul (2007a), The ejection-sweep cycle over bare and forested gentle hills: A laboratory experiment, *Boundary Layer Meteorol.*, 122(3), 493–515, doi:10.1007/s10546-006-9117-x.
- Poggi, D., and G. G. Katul (2007b), Turbulent flows on forested hilly terrain: The recirculation region, *Q. J. R. Meteorol. Soc.*, 133(625), 1027–1039, doi:10.1002/qj.73.
- Poggi, D., and G. G. Katul (2007c), An experimental investigation of the mean momentum budget inside dense canopies on narrow gentle hilly terrain, *Agric. For. Meteorol.*, 144(1–2), 1–13, doi:10.1016/j.agrformet.2007.01.009.
- Poggi, D., and G. G. Katul (2008a), The effect of canopy roughness density on the constitutive components of the dispersive stresses, *Exp. Fluids*, 45(1), 111–121, doi:10.1007/s00348-008-0467-7.
- Poggi, D., and G. G. Katul (2008b), Micro- and macro-dispersive fluxes in canopy flows, *Acta Geophys.*, 56(3), 778–799, doi:10.2478/s11600-008-0029-7.
- Poggi, D., G. G. Katul, and J. D. Albertson (2004a), A note on the contribution of dispersive fluxes to momentum transfer within canopies—Research note, *Boundary Layer Meteorol.*, 111(3), 615–621, doi:10.1023/B:BOUN.0000016563.76874.47.
- Poggi, D., G. G. Katul, and J. D. Albertson (2004b), Momentum transfer and turbulent kinetic energy budgets within a dense model canopy, *Boundary Layer Meteorol.*, 111(3), 589–614, doi:10.1023/B:BOUN.0000016502.52590.af.

- Poggi, D., A. Porporato, L. Ridolfi, J. D. Albertson, and G. G. Katul (2004c), The effect of vegetation density on canopy sub-layer turbulence, *Boundary Layer Meteorol.*, *111*(3), 565–587, doi:10.1023/B:BOUN.0000016576.05621.73.
- Poggi, D., G. G. Katul, J. D. Albertson, and L. Ridolfi (2007), An experimental investigation of turbulent flows over a hilly surface, *Phys. Fluids*, *19*(3), 036601, doi:10.1063/1.2565528.
- Pokrajac, D., L. J. Campbell, V. Nikora, C. Manes, and I. McEwan (2007), Quadrant analysis of persistent spatial velocity perturbations over square-bar roughness, *Exp. Fluids*, *42*(3), 413–423, doi:10.1007/s00348-006-0248-0.
- Raupach, M. R. (1992), Drag and drag partition on rough surfaces, *Boundary Layer Meteorol.*, *60*(4), 375–395, doi:10.1007/BF00155203. (Correction, *Boundary Layer Meteorol.*, *76*(3), 303–304, doi:10.1007/BF00709356, 1995)
- Raupach, M. R. (1994), Simplified expressions for vegetation roughness length and zero-plane displacement as functions of canopy height and area index, *Boundary Layer Meteorol.*, *71*(1–2), 211–216, doi:10.1007/BF00709229.
- Raupach, M. R., and R. H. Shaw (1982), Averaging procedures for flow within vegetation canopies, *Boundary Layer Meteorol.*, *22*(1), 79–90, doi:10.1007/BF00128057.
- Raupach, M. R., J. J. Finnigan, and Y. Brunet (1996), Coherent eddies and turbulence in vegetation canopies: The mixing-layer analogy, *Boundary Layer Meteorol.*, *78*(3–4), 351–382, doi:10.1007/BF00120941.
- Shi, Z., J. S. Pethick, and K. Pye (1995), Flow structure in and above the various heights of a salt-marsh canopy—A laboratory flume study, *J. Coastal Res.*, *11*(4), 1204–1209.
- Shimizu, Y., and T. Tsuiumoto (1994), Numerical analysis of turbulent open-channel flow over a vegetation layer using a k-epsilon turbulence model, *J. Hydrosoci. Hydraul. Eng.*, *11*, 57–67.
- Stone, B. M., and H. T. Shen (2002), Hydraulic resistance of flow in channels with cylindrical roughness, *J. Hydraul. Eng.*, *128*(5), 500–506, doi:10.1061/(ASCE)0733-9429(2002)128:5(500).
- Thom, A. S. (1971), Momentum absorption by vegetation, *Q. J. R. Meteorol. Soc.*, *97*(414), 414–428, doi:10.1002/qj.49709741404.
- Tsihrintzis, V. A., and E. E. Madiedo (2000), Hydraulic resistance determination in marsh wetlands, *Water Resour. Manage.*, *14*, 285–309, doi:10.1023/A:1008130827797.
- White, B. L., and H. M. Nepf (2008), A vortex-based model of velocity and shear stress in a partially vegetated shallow channel, *Water Resour. Res.*, *44*, W01412, doi:10.1029/2006WR005651.
- Wilson, C. A. M. E., and M. Horritt (2002), Measuring the flow resistance of submerged grass, *Hydrol. Processes*, *16*, 2589–2598, doi:10.1002/hyp.1049.
- Wilson, C., T. Stoesser, P. D. Bates, and A. B. Pinzen (2003), Open channel flow through different forms of submerged flexible vegetation, *J. Hydraul. Eng.*, *129*(11), 847–853, doi:10.1061/(ASCE)0733-9429(2003)129:11(847).
- Wu, F.-C., H. W. Shen, and Y.-J. Chou (1999), Variation of roughness coefficients for un-submerged and submerged vegetation, *J. Hydraul. Eng.*, *125*(9), 934–942, doi:10.1061/(ASCE)0733-9429(1999)125:9(934).

---

G. G. Katul and C. Krug, Department of Civil and Environmental Engineering, Duke University, P.O. Box 90287, Durham, NC 27708-0287, USA.

D. Poggi, Dipartimento di Idraulica, Trasporti ed Infrastrutture Civili, Politecnico di Torino, I-10129 Torino, Italy. (davide.poggi@polito.it)